2011

Population dynamics and niche distribution of uropathogenic Escherichia coli during acute and chronic urinary tract infection

Drew J. Schwartz
Washington University School of Medicine in St. Louis

Swaine L. Chen
National University of Singapore

Scott J. Hultgren
Washington University School of Medicine in St. Louis

Patrick C. Seed
Duke University

Infection and Immunity

Population Dynamics and Niche Distribution of Uropathogenic Escherichia coli during Acute and Chronic Urinary Tract Infection

Drew J. Schwartz, Swaine L. Chen, Scott J. Hultgren and Patrick C. Seed

Infect. Immun. **2011, 79(10):4250. DOI: 10.1128/IAI.05339-11. Published Ahead of Print 1 August 2011.**

INFECTION AND IMMUNITY, Oct. 2011, p. 4250–4259 Vol. 79, No. 10
0019-9567/11/$12.00 doi:10.1128/IAI.05339-11

Population Dynamics and Niche Distribution of Uropathogenic *Escherichia coli* during Acute and Chronic Urinary Tract Infection▽†

Drew J. Schwartz,[1] Swaine L. Chen,[2] Scott J. Hultgren,[1]* and Patrick C. Seed[3]*

Department of Molecular Microbiology and Microbial Pathogenesis, Center for Women's Infectious Disease Research, Box 8230, Washington University School of Medicine, 660 S. Euclid Ave., St. Louis, Missouri 63110[1]; Department of Medicine, Division of Infectious Diseases, Yong Loo Lin School of Medicine, National University of Singapore, and Infectious Diseases Group, Genome Institute of Singapore, 60 Biopolis Street, Genome #02-01, Singapore 138672[2]; and Departments of Pediatrics, Molecular Genetics, and Microbiology, Box 103100, Duke University School of Medicine, Durham, North Carolina 27710[3]

Received 5 May 2011/Returned for modification 3 June 2011/Accepted 26 July 2011

Urinary tract infections (UTIs) have complex dynamics, with uropathogenic *Escherichia coli* (UPEC), the major causative agent, capable of colonization from the urethra to the kidneys in both extracellular and intracellular niches while also producing chronic persistent infections and frequent recurrent disease. In mouse and human bladders, UPEC invades the superficial epithelium, and some bacteria enter the cytoplasm to rapidly replicate into intracellular bacterial communities (IBCs) comprised of ~10^4 bacteria each. Through IBC formation, UPEC expands in numbers while subverting aspects of the innate immune response. Within 12 h of murine bladder infection, half of the bacteria are intracellular, with 3 to 700 IBCs formed. Using mixed infections with green fluorescent protein (GFP) and wild-type (WT) UPEC, we discovered that each IBC is clonally derived from a single bacterium. Genetically tagged UPEC and a multiplex PCR assay were employed to investigate the distribution of UPEC throughout urinary tract niches over time. In the first 24 h postinfection (hpi), the fraction of tags dramatically decreased in the bladder and kidney, while the number of CFU increased. The percentage of tags detected at 6 hpi correlated to the number of IBCs produced, which closely matched a calculated multinomial distribution based on IBC clonality. The fraction of tags remaining thereafter depended on UTI outcome, which ranged from resolution of infection with or without quiescent intracellular reservoirs (QIRs) to the development of chronic cystitis as defined by persistent bacteriuria. Significantly more tags remained in mice that developed chronic cystitis, arguing that during the acute stages of infection, a higher number of IBCs precedes chronic cystitis than precedes QIR formation.

Population bottlenecks exist for many infections and are particularly well documented during transmission between hosts for RNA viruses and parasites (1, 3, 27, 28, 35, 41). Localizing bottlenecks in time and space during an infection can identify steps in pathogenesis where an organism encounters the strongest barriers to establishing a foothold within a host. Bottlenecks may also represent important steps in host colonization and pathogenesis to target with therapeutics. Similar studies have been undertaken to identify genes important for tissue colonization and transit between tissues for bacterial pathogens (7, 36, 37). Several potential bottlenecks limiting the progression of uropathogenic *Escherichia coli* (UPEC) to later stages of infection exist in the pathogenic cascade of urinary tract infections (UTIs): (i) invasion of the superficial bladder epithelium, (ii) avoidance of Toll-like receptor 4 (TLR4)-mediated expulsion (46), (iii) persistence in the face of superficial facet cell exfoliation, (iv) the maturation process of intracellular bacterial communities (IBCs), (v) ascension from bladder to the kidneys, and (vi) possible descent from kidneys to the bladder. These population dynamics all occur in the face of clearance mechanisms, including micturition and the innate immune system (38). Understanding these bottlenecks in the setting of mucosal infection of the urinary tract will provide insight into the pathogenesis of this complex infection with the goal to develop better treatments.

UTIs are painful, expensive to the individual and society, and will affect 50% of women during their lifetime (12). The vast majority of community-acquired UTIs are caused by UPEC. The clinical diagnosis of UTI hinges upon the ability to culture bacteria from clean-catch urine samples. When the uropathogen is sensitive to the chosen agent, oral antibiotics typically produce a rapid improvement in symptoms and sterilization of the urine (15, 16). Despite appropriate treatment of a primary UTI, 25 to 40% of adult women will have at least one recurrence (rUTI) within 6 months of her initial infection (33, 45). Additionally, up to 20% of women may experience the symptoms of cystitis, or infection of the bladder, with accompanying urine cultures from clean-catch specimens below the diagnostic cutoff of $<10^5$ CFU/ml (13). This implies that bacterial occupation of urinary tract niches even in the absence of clinical diagnosis can contribute to symptoms of UTI. The exact location of bacteria within the urinary tract in these

* Corresponding author. Mailing address for P. C. Seed: Departments of Pediatrics, Molecular Genetics, and Microbiology, Box 103100, Duke University School of Medicine, Durham, NC 27710. Phone: (919) 684-9590. Fax: (919) 681-2089. E-mail: Patrick.seed@duke.edu. Mailing address for S. J. Hultgren: Department of Molecular Microbiology and Microbial Pathogenesis, Center for Women's Infectious Disease Research, Box 8230, Washington University School of Medicine, 660 S. Euclid Ave., St. Louis, MO 63110. Phone: (314) 362-6772. Fax: (314) 362-1998. E-mail: Hultgren@borcim.wustl.edu.

† Supplemental material for this article may be found at http://iai.asm.org/.

▽ Published ahead of print on 1 August 2011.

syndromes is, at present, unknown. The high prevalence of UTI, frequent repeated antibiotic therapy for rUTI, and the failure to use stringent diagnoses of UTI may drive rising antibiotic resistance (15–17). Through a thorough examination of the molecular basis for rUTI and the identification of the major persistent reservoirs for UPEC within the urinary tract, new therapeutic strategies may be designed to eliminate UPEC from the urinary tract and thus better guide appropriate antibiotic usage.

Current knowledge of the pathogenesis of UPEC UTI is incomplete, but accumulated molecular studies demonstrate tremendous complexity in the pathogenesis of the disease. In most primary UTIs, UPEC is thought to ascend the urethra from the perineum to colonize the bladder lumen. Additionally, UPEC can ascend the ureters and colonize the kidneys. Increased vesicoureteral reflux (VUR) enhances the likelihood of bacterial ascension into the kidneys and subsequent renal scarring in children and individuals with neurogenic bladders (32). Through studies in a murine model of UTI, several novel intracellular pathways within the bladder important for UPEC pathogenesis have been elucidated. After experimental transurethral inoculation of UPEC into the urinary tract, UPEC invades the superficial facet cells of the bladder in a type 1 pilus-dependent manner (29, 34, 38). In order to evade expulsion from these cells via a TLR4-dependent mechanism (46), UPEC must escape into the cell cytoplasm, where it rapidly replicates and aggregates into cytosolic clusters of bacteria called intracellular bacterial communities (IBCs), a process that occurs independent of specific host genotypes (2, 14). After full maturation of the IBCs, UPEC becomes filamentous and flux out of the superficial facet cell in response to a TLR4-dependent host signal (25). The luminal bacteria may then invade other superficial facet cells, renewing the invasion and intracellular replication cascade (24, 25). Thus, UPEC undergoes at least two rounds of IBC formation over the first 24 h postinfection (hpi). Occupation of an intracellular niche by UPEC is not unique to the mouse model, as IBCs and filamentous bacteria have been frequently identified in urine from women with acute cystitis (42). Replication within epithelial cells may protect UPEC from being cleared by neutrophils, antimicrobial peptides, micturition, and antibiotic administration (4, 25). In the C3H/HeN mouse model of UTI, the IBC stage is most active during the first 24 hpi (24). Thus, during UTI, many niches within the urinary tract are colonized, including the bladder lumen, cells of the bladder epithelium, and the kidneys.

IBCs are not typically observed in C3H/HeN mice after 48 hpi. However, outcomes of the infection are dependent on the immune response to acute events (20). The C3H/HeN mouse model of UTI recapitulates several of the outcomes present in humans. The outcome of bladder infection in these mice is bimodal, with 20 to 40% of infected C3H/HeN mice developing persistent bacteriuria and chronic cystitis (20). Placebo-controlled trials have demonstrated persistent bacteriuria in women with or without resolution of symptoms in the absence of antibiotic treatment (11, 33). High levels of interleukin 5 (IL-5), IL-6, keratinocyte cytokine (KC), and granulocyte colony-stimulating factor (G-CSF) in the serum of C3H/HeN mice at 24 hpi are nearly 100% predictive of ensuing chronic cystitis (20). The remaining mice have low levels of these cytokines and resolve the acute infection, evidenced by sterile urine. However, even upon resolution of bacteriuria, UPEC may occupy niches in the underlying epithelium in quiescent intracellular reservoirs (QIRs) (40). Thus, UTI pathogenesis has complexity in both space (tissue niche) and time. During the acute stages of pathogenesis, IBC formation facilitates the expansion of bacterial numbers in the face of innate defenses. A multitude of consequences to the acute events exist, ranging from resolution of infection with or without accompanying QIRs to ensuing chronic cystitis or pyelonephritis. The relationship between IBC formation during acute infection and the subsequent outcome of infection is not known. The dynamics of acute infection and the subsequent outcomes may also be altered if the kidneys are infected concurrently with the bladder. Underlying conditions, such as vesicoureteral reflux (VUR), increase the likelihood of coinfection of the kidneys and bladder. These complicated population dynamics may be modeled in specific mouse strains, such as C3H/HeN. These mice are also susceptible to kidney infection due to a high rate of VUR (21, 22, 43, 47).

With all of the transitions UPEC makes between anatomic and cellular spaces, it is likely that only a fraction of the total bacterial population transitions from one niche to another, in which case population bottlenecks likely occur. Based on the complexity of UTI and the various niches UPEC inhabits during infection, we sought to determine transit between relevant niches and barriers within the urinary tract over time and whether the penetration of infection barriers resulted in an expansion of those descendants. A prior study indicated that intracellular UPEC makes up a significant proportion of the bacteria in the bladder during the first 48 hpi, as determined by *ex vivo* gentamicin protection assays (38). Early in infection, micturition and neutrophil influx may disproportionately reduce or eliminate luminal bacteria, while intracellular UPEC is largely protected from these clearance mechanisms.

We addressed the role of bottlenecks in UPEC population dynamics during UTI using a panel of 40 unique genetically tagged isogenic UPEC isolates that were tracked using a multiplex PCR assay. We modeled the dynamics of population flux using a calculated multinomial distribution and compared theoretical values to a complicated model of infection using the C3H/HeN mouse, which is susceptible to VUR, thus resulting in UPEC being distributed during acute infection in the bladder and kidneys. In the bladder, we demonstrated that each IBC arises from replication of a single invasive bacterium and that the number of IBCs present at 6 hpi strongly correlates with the number of unique tags present. In mice that would likely resolve bacteriuria and/or develop QIRs, the fraction of uniquely tagged UPEC decreased to 10 to 20% of the number of tags present in the initial inoculum during the first 24 hpi in whole-bladder specimens. In contrast, in mice with persistent bacteriuria, a hallmark of chronic cystitis, nearly 60% of unique tags remained. Thus, a high number of IBCs formed at 6 hpi and/or an inability to clear bacteria from the bladder lumen preceded chronic cystitis. Utilizing *ex vivo* gentamicin protection assays to separate intracellular and extracellular bladder populations, we found that during acute UTI, the majority of remaining clones occupied all niches within the urinary tract, while later in infection disparate clonal populations existed independently in the bladders or kidneys.

MATERIALS AND METHODS

Construction of 40 isogenic tagged UPEC isolates. Unique tags were inserted into the chromosome following the *ybhC* gene in the region of the lambda phage attachment site of the clinical isolate UTI89 (39). This site was chosen since prior insertions in this region (*gfp* reporter fusions) did not adversely affect pathogenesis (49). The tags were designed using unique sequences as reported by Lehoux et al. (30, 31). Primer sequences are shown in Table S1 in the supplemental material. For the construction of the genomic insertion cassettes, the chloramphenicol or kanamycin cassette from pKD3 or pKD4 (10) was amplified using primer BP-1 in combination with BP-2A, BP-2B, and BP-2C. The respective products were digested with EcoRI and column purified (Qiagen). Each of the BP-00F primers was phosphorylated in a reaction that included 1× T4 ligase buffer (NEB), 10 mM dATP (Promega), and 1 U of T4 polynucleotide kinase (Invitrogen) for 30 min at 37°C. The appropriate BP-00F and BP-00R primers were annealed by mixing equal molar ratios in distilled water (dH_2O), heating to 95°C for 5 min, and cooling slowly to room temperature (RT). In a similar method, primers BP-5 and BP-6 were annealed to each other. A tripartite ligation was performed using the BP-1/BP-2-digested PCR products with the annealed products of BP-00F/R and BP-5/BP-6 in 1× T4 ligase buffer and 10 U of T4 ligase for 1 h at RT. To a PCR mixture containing 1× Pfx buffer (Invitrogen), 2 mM $MgSO_4$, 0.2 mM deoxynucleoside triphosphate (dNTP), 2.5 U of Pfx polymerase (Invitrogen), 200 pmol each of primers BP-1 and BP-6, and 0.5 μl of each ligation were added. The reactions were cycled at 94°C for 3 min followed by 30 cycles of 94°C for 15 s, 55°C for 45 s, and 68°C for 1.5 min. A final extension at 68°C for 7 min was performed. The ~1.6-kb products were verified by gel electrophoresis and column purified (Qiagen). Chromosomal insertion of the tag constructs was performed using the Red recombinase method (10). The tags were verified by colony PCR in a reaction mixture containing 1 × PCR buffer (Invitrogen) with 0.2 mM dNTP, 2.5 mM $MgCl_2$, 2.5 U *Taq* polymerase (Invitrogen), and 200 pmol each of the appropriate primer pairs, BP-8K (kanamycin template) or BP-8C (chloramphenicol template) and BP-00F. Growth curves of each individual strain were performed to ensure no gross growth defects in broth culture (data not shown).

Evaluation of isogenic UPEC strains in a murine cystitis model. In preparation for inoculation into mice, each of the 40 isogenic UTI89 derivatives was grown individually in LB statically at 37°C overnight and then subcultured 1:1,000 into 2 ml of fresh LB with static growth at 37°C for 18 to 24 h. Cell density was measured using an optical density at 600 nm (OD_{600}) value, and each clone was added in approximately equal cell numbers to a central pool. The pooled bacteria were centrifuged for 10 min at 6,500 × *g* at 4°C. The pellet was resuspended in 20 to 25 ml of sterile phosphate-buffered saline (PBS) to yield a final cell suspension in which 50 μl contained ~1×10^7 to 2×10^7 CFU. Fifty microliters was introduced over 10 s into 7- to 8-week-old C3H/HeN mice under 2.5% isofluorane inhalation via a transurethral route. The infections were allowed to proceed for 1 h to up to 4 weeks, at which time the mice were sacrificed under anesthesia, and the bladders and kidneys were removed and homogenized in 1 ml and 0.800 ml sterile PBS, respectively. Homogenates were serially diluted and plated to enumerate the bacteria in the tissues. Genomic DNA was obtained from the bacterial lawns by the addition of 2 ml of sterile water in each petri dish and scraped using a bacterial cell scraper (BD Falcon). The bacteria were pelleted by centrifugation and washed with PBS. The final pellet was processed using the Promega genomic DNA isolation kit per the manufacturer's instructions. Genomic DNA was also prepared from a bacterial pellet of the pooled input inoculum.

BAR-PATH multiplex PCR was performed using 50 ng of genomic DNA in a PCR mix, including 1× *Taq* buffer (Invitrogen), 2.5 mM $MgCl_2$, 0.2 mM dNTP, 100 pmol each of BP-8C and BP-8K, and 2.5 U *Taq* DNA polymerase (Invitrogen). The BP-00F primers (see Table S1 in the supplemental material) were mixed in sets of 3 primers for inclusion in PCRs (BP-01F, BP-02F, BP-03F and BP-04F, BP-05F, BP-06F, etc.) and added to the reaction mixture at final concentrations of ~66.6 pmol/primer. Reactions were cycled with a hot start and then at 94°C for 3 min followed by touchdown PCR with 10 cycles of 94°C for 30 s, 62°C for 30 s with a 1°C decrease per cycle, and 72°C for 30 s. Next, 30 cycles were performed at 94°C for 15 s, 55°C for 15 s, and 72°C for 30 s. A final 7-min extension at 72°C was performed. Ten microliters of the 25 μl reaction was run on a 2.5% Tris-borate-EDTA (TBE)-agarose gel. The presence or absence of an individual strain in the multiplex PCR was determined by eye in comparison to the intensity of its cognate band in the inoculum. If a strain was not detected in the inoculum pool, it was not included in the analysis for that experiment. Thirty-seven of the 40 tags were routinely detected in the inoculum. Three tags were statistically underrepresented in the PCR of the inoculum pool and were thus excluded in the subsequent analyses of the endpoint samples. Ambiguous bands were analyzed in an independent multiplex PCR replicate. All mouse infection studies were approved by the Animal Studies Committee of Washington University in St. Louis, MO.

IBC enumeration. To quantify the number of IBCs per bladder, bladders were bisected and splayed onto sterile silica plates and fixed with 3% paraformaldehyde (Sigma). The bladders were washed 3 times with 2 mM $MgCl_2$ (Sigma), 0.01% Na deoxycholate (Sigma), and 0.02% Nonidet P-40 (Roche) in sterile PBS, pH 7.4. Bladders were then stained in 0.4 ml of 25 mg/ml X-Gal (5-bromo-4-chloro-3-indolyl-β-D-galactopyranoside; Sigma) and a solution containing 1 mM potassium ferrocyanide and 1 mM potassium ferricyanide (Sigma). After incubating at 30°C for 16 h, bladders were visualized under a dissecting microscope, where IBCs appeared as bright blue punctate circles.

Confocal laser scanning microscopy. Female 6- to 7-week-old C3H/HeN mice were infected with a 1:1 or 1:50 mixture of UTI89 and UTI89::HKGFP and sacrificed at 6 or 12 hpi (49). Bladders were extracted, splayed, and counterstained with TO-PRO-3 and imaged with a Zeiss LSM410 confocal laser scanning microscope.

***Ex vivo* gentamicin protection assay.** At the indicated times postinfection, bladders were removed aseptically and bisected twice. The bladders were washed three times with 500 μl sterile PBS. The washes were pooled, spun at 500 rpm for 5 min, and dilution plated as described earlier. This wash was termed "luminal" or "extracellular." The bladders were then incubated for 90 min with 100 μg/ml gentamicin to kill adherent extracellular bacteria. After this incubation, the bladders were washed twice with 1 ml sterile PBS. The bladder was then homogenized in 1 ml sterile PBS and dilution plated to enumerate intracellular CFU. Bacterial pellets were obtained and processed as described earlier.

RESULTS

IBCs arise from a single invasive bacterium. UPEC invades the superficial facet cells of the bladder 15 min to 1 h postinoculation into the urinary tract as determined by *ex vivo* gentamicin protection assays (48). Over the next 8 to 12 h, IBC formation ensues for bacteria that have successfully invaded and escaped into the cytosol of the superficial facet cells (24). To address whether IBCs contain a clonal population expanded from a single bacterium or an aggregate of multiple distinct founders, we performed coinfections of mice with 1:1 and 50:1 ratios of unlabeled and green fluorescent protein (GFP)-marked isogenic UPEC (49). Six hours postinfection, mice were euthanized, and the bladders were splayed, fixed, and stained with TO-PRO-3 and examined by confocal microscopy. As a result, the unlabeled UPEC IBCs appeared red and the GFP-marked UPEC IBCs appeared yellow-green. Of the approximately 500 IBCs examined, each was exclusively red or yellow-green, regardless of the inoculation ratio (Fig. 1). When superficial facet cells contained more than one IBC derived from a different inoculating strain, a clear demarcation existed such that no bacterial mixing occurred (Fig. 1C and D), indicating that IBCs are clonal formations arising from a single invasive bacterium.

Formation of IBCs strongly correlates to tag diversity. Given that each IBC is derived from a single bacterial founder and IBC formation is rare, with only 0.01 to 0.001% of the initial inoculum successfully undergoing IBC formation, we anticipated that various bottlenecks restricting invasion and subsequent IBC formation may result in a significant founder effect in later stages of infection. At 6 hpi following an initial inoculation of 1×10^7 to 5×10^7 UPEC CFU, each mouse bladder contained between 3 and 700 IBCs (median, 49.5; geometric mean, 40) (Fig. 2), consistent with previously reported data for C3H/HeN mice (5, 8, 44). Combining prior knowledge that the bacterial population is primarily intracellular at 12 hpi (38, 39) with the finding that IBCs are clonal, we

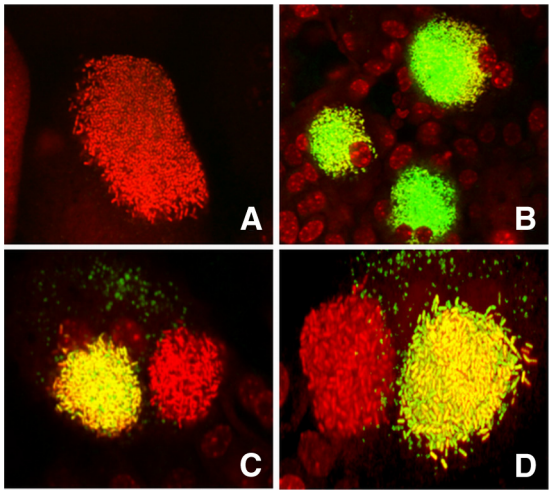

FIG. 1. IBCs are clonal and derived from a single invasive bacterium. C3H/HeN mice were coinfected with UTI89 and UTI89::HKGFP and sacrificed at 6 hpi and 12 hpi. Bladders were aseptically removed, splayed, and imaged with confocal microscopy. (A and B) IBCs in whole mount at 6 hpi, counterstained with TO-PRO-3. Each image shows the merged red and green channel data. (C and D) Coresident IBCs inside a single superficial facet cell at 12 hpi. Representative images of over 500 independent IBCs are shown.

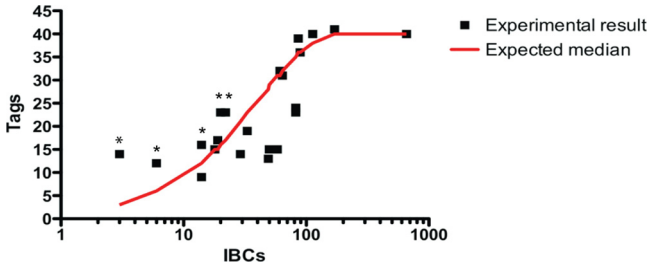

FIG. 2. IBC number correlates with the number of tags present. C3H/HeN mice were infected as described and processed to enumerate IBCs and extract bacterial genomic DNA (see Materials and Methods). Black squares represent the number of IBCs and the number of tagged strains present per mouse bladder. The line is the median number of tags expected based on a multinomial distribution of IBC number (see Discussion and the supplemental material). Data represent 3 independent experiments, with 5 to 10 mice per experiment. *, bladders with a greater number of tags than IBCs.

hypothesized that the invasion and IBC formation cycle acts as a strong population bottleneck that restricts overall bacterial diversity and may subsequently contribute a significant proportion of bacteria populating later stages of infection. In order to test this hypothesis, we designed 40 isogenic strains of UTI89, each with a unique 100- to 300-bp genetic sequence inserted into the λ phage region of the genome (see Materials and Methods). Bacteria containing these unique tags were identified using 8 multiplex PCRs. We reasoned that the small number of clonal IBCs relative to the total inoculum, which was primarily intracellular by 12 hpi (38), may contribute to a founder effect in the number of unique genotypes arising from this early bottleneck event.

We infected mice with a pool of the tagged strains in equal proportions. At 6 hpi, the mice were sacrificed and the infected bladders were splayed and stained with X-Gal to detect bacterial beta-galactosidase and thus localize UPEC in mature IBC formations, which stained punctate purple. Following enumeration of IBCs, the bladders were homogenized, and genomic DNA was extracted from the bacteria present in the bladder. We found a broad range of unique bacterial signatures corresponding to the range of IBCs formed per bladder at 6 hpi (Fig. 2, black squares). Based on the hypothesis that the bacteria contained in IBCs account for the majority of bacteria in the bladder at 6 hpi, we calculated the fraction of tags that most likely would be remaining relative to the number of IBCs present using a multinomial distribution (Fig. 2, line). Superimposition of the theoretical multinomial distribution onto the experimental data revealed a close fit (see Discussion and the supplemental material). The five data points marked with asterisks in Fig. 2 represent bladders that contained more tags than IBCs. The increased fraction of tags in these bladders likely represented invasion events of bacteria that had not yet replicated into a mature IBC and thus not yet discerned in the X-Gal-stained bladders but were detected by the more sensitive multiplex PCR assay. For mice whose bladders contained >100 IBCs at 6 h, all 40 tags were present. These data suggest that early in infection, the clonal IBC populations, arising from a small number of bacterial founders, may contribute the majority of bacterial diversity to later stages of infection.

Bacterial diversity decreased dramatically in the bladders and kidneys over time. During the most acute stages of isolated cystitis, the formation of IBCs, each from a single invasive bacterium and coincident with luminal clearance of bacteria, would be anticipated to constitute a stringent bottleneck, limiting the genetic diversity of organisms progressing to later stages of infection. We first determined the overall dynamics of infection using our set of 40 uniquely tagged UPEC strains as a proxy for bacterial diversity to understand the occupation of the urinary tract over time. We infected C3H/HeN mice with 1×10^7 to 5×10^7 total CFU (2.5×10^5 to 1.25×10^6 CFU/unique strain) and tracked them over the course of 4 weeks. At the designated times after infection, the bladders and kidneys were homogenized, and 6% of the sample was plated to enumerate CFU (Fig. 3A and B). Through this approach, rare abundance tags are likely amplified to above the limit of detection in the multiplex PCR assay. A tag comprising <20 CFU in the sample could potentially be lost with this method, but such rare abundance tags are not likely to persist within the urinary tract for an extended period of time.

Total bacterial diversity in the bladder decreased significantly over the first 24 hpi ($P = 0.003$, 1 hpi versus 24 hpi) to a median plateau of 25 to 40% of the initial tags remaining (Fig. 3C), while the number of CFU increased over this same time period to 10^5 CFU (Fig. 3A). The simultaneous reduction in tag diversity with an increase in the number of CFU occurred during the time in which IBCs formed, suggesting a relationship between the IBC bottleneck and a founder effect in populating the bladder. Bacterial diversity in the kidneys also decreased over this same time span ($P = 0.003$, 1 hpi versus 24 hpi), with approximately the same fraction of tags present in the bladders and kidneys by 1 week postinfection (wpi) (Fig. 3D).

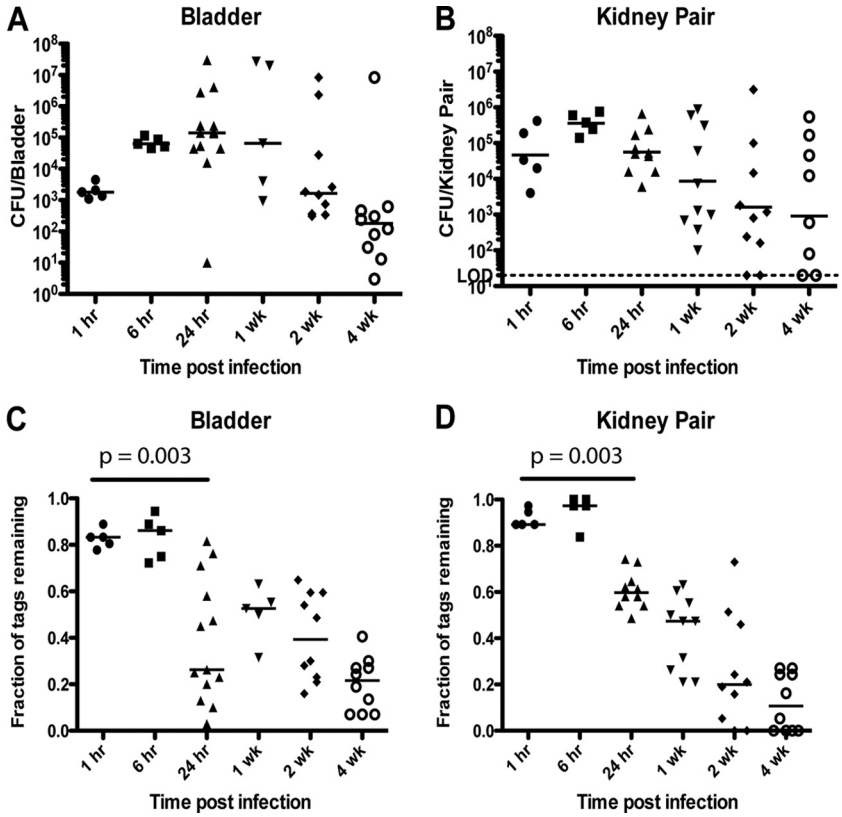

FIG. 3. Bacterial diversity decreased dramatically during the first 24 hpi. At the indicated times postinfection, C3H/HeN mice were sacrificed, the bladder and kidneys were removed aseptically and homogenized in PBS, and 6% of the homogenate was plated to enumerate CFU in the bladders (A) and kidney pairs (B). Genomic DNA was isolated from a lawn of UPEC isolated from the tissue homogenates, and multiplex PCR was conducted to determine the fraction of the 40 unique tags present in each bladder (C) and kidney pair (D). CFU data are presented as CFU/whole organ. Bars are median values. n = 1 to 2 experiments, with 5 to 8 mice each. P values were calculated using a two-tailed Mann-Whitney nonparametric comparison. An initial experiment conducted with 43 tags is also included in this analysis.

IBC formation correlates with the outcome of infection. In C3H/HeN mice, the fate of disease is determined within the first 24 h of infection (20). The two disease outcomes of resolution of bacteriuria concomitant with the establishment of QIRs and the development of persistent bacteriuria indicative of chronic cystitis result in a bimodal distribution of bacterial CFU within the bladder that occurs after 1 week (22). Thus, we investigated the relationship between the number of IBCs formed early in infection and the impact on the fraction of tags remaining later in infection and disease outcome (20, 40).

We infected 20 mice with equal proportions of the 40 uniquely tagged UTI89 strains and determined the number of bacterial CFU and the number of unique tags that remained at 2 wpi. Mice were stratified based on their urine titers over time and their 2-wpi bladder titers. Chronic cystitis was categorized by persistent bacteriuria of $>10^4$ CFU/ml at 1, 3, 7, 10, and 14 dpi and a 2-wpi bladder titer of $>10^4$ CFU (20). The remaining mice were classified based on bladder titers of $<10^4$ CFU and at least one urine collection over the 2-week infection that contained $<10^4$ CFU/ml UPEC (Fig. 4A and B). Mice that developed persistent bacteriuria and chronic cystitis had significantly more unique UPEC signatures present in the bladder by 2 wpi than mice that resolved infection (Fig. 4C). Based on the founder effect theory, this would argue that development of chronic cystitis is correlated with increased IBC formation during the acute stage of infection, which is consistent with the strong correlation between IBC formation and the fraction of tags present throughout the bladder during the IBC cycle (Fig. 2). Conversely, decreased IBC formation is more likely correlated with resolution of bacteriuria with reservoir bladder titers of $<10^4$ CFU.

Population dynamics in acute versus chronic infection. UTI is a dynamic infection sometimes entailing concomitant kidney infection. Populations of UPEC within the bladders and kidneys of C3H/HeN mice may thus be shaped by different independent environmental forces, including unique bottlenecks. These physically separated populations may subsequently intermix to generate some intermediate, combined population. Abundant influx of neutrophils and immune mediators into the bladder occurs very early during UTI in both mice and humans (21, 23, 26). Invasion of the bladder epithelium may represent a mechanism for UPEC to increase its population during UTI while remaining separated from much of the innate immune response. Gentamicin protection assays on *ex vivo*-infected bladders support this concept, demonstrating that by 12 hpi in murine UTI, the majority of UPEC CFU is intracellular (38). On the basis of these prior studies, we sought to determine the location of UPEC within urinary tract niches throughout infection. In order to obtain a more complete understanding of how bacterial subpopulations are distributed within the urinary

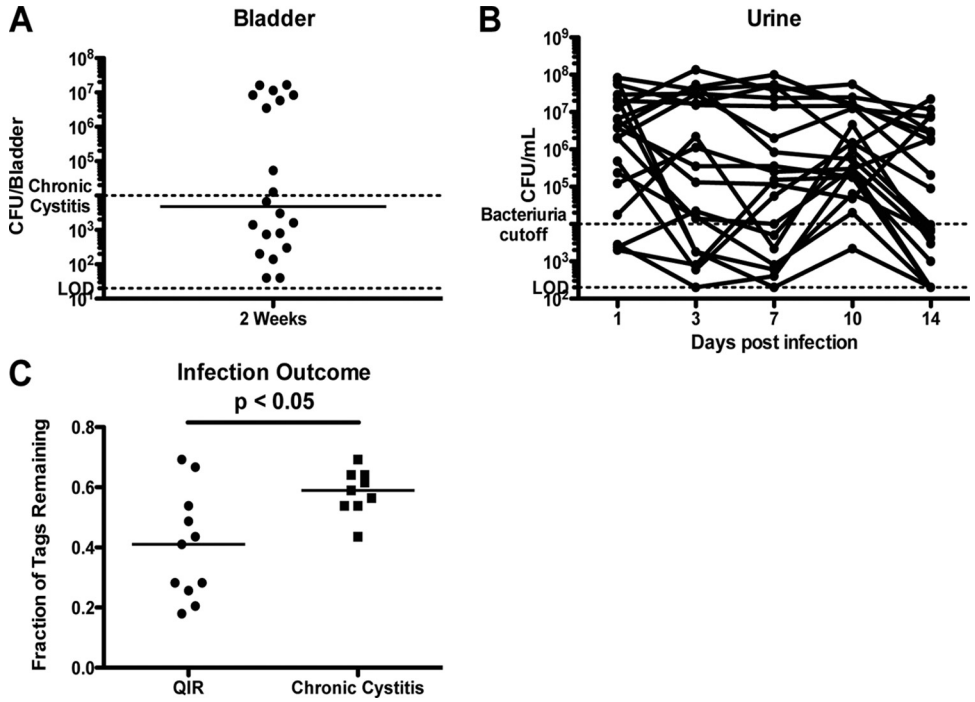

FIG. 4. Higher fraction of unique bacterial signatures remains in mice experiencing chronic cystitis. (A) Two weeks postinfection, C3H/HeN mice were sacrificed, and the bladders were removed aseptically, homogenized, and plated to enumerate CFU. (B) Urine samples were obtained by gentle suprapubic pressure and plated to enumerate CFU. The dashed line at 10^4 CFU represents the limit for assessing the presence of UTI in clean-catch urine samples (40). Urine titers above this point are considered bacteriuria indicative of a UTI, while bladder titers greater than this cutoff indicate chronic cystitis. (C) Genomic DNA was then obtained from the bacteria from each bladder sample, and multiplex PCR was conducted. Bars are median values. *P* values were calculated using a two-tailed Mann-Whitney nonparametric comparison.

tract at a given time, sampling of different niches within the urinary tract was performed using mice infected with equal numbers of each of the 40 genetically tagged UTI89 strains at different times postinfection. We obtained clean-catch urine from mice by gentle suprapubic pressure and plated it to enumerate CFU (Fig. 5A). Afterwards, the mice were sacrificed, and the bladder was bisected twice and washed with sterile PBS to liberate loosely bound and planktonic UPEC CFU, heretofore referred as the "luminal" or "extracellular" fraction (Fig. 5B). The intact, quadrisected bladder was incubated with the antibiotic gentamicin, which does not penetrate the bladder epithelium, thus selectively eliminating extracellular organisms. After the gentamicin was washed away, the bladder tissue was homogenized to liberate the intracellular bacteria, designated the "gentamicin-protected bladder" population (Fig. 5C). During the first 24 hpi, this fraction represented bacteria that invaded superficial facet cells and were, in some cases, within IBCs. After 48 hpi, when IBC formation no longer occurs, the gentamicin-protected fraction consisted of bacteria within QIRs or another niche protected from gentamicin. Kidneys were also homogenized and plated to enumerate CFU (Fig. 5D).

All of the 40 uniquely tagged UPEC strains were present in both the extracellular and intracellular populations at 1 hpi (Fig. 5F and G). This amount of tag diversity was not statistically different from that observed in the whole bladder at 1 hpi (Fig. 3C; $P > 0.05$, Wilcoxon signed-rank test; hypothetical median = 1.0). At 6 hpi, the proportion of genetic tags approached 1 in the kidneys, likely due to VUR of the inoculum in the C3H/HeN mice at the initiation of the infection. However, the proportion of genetic tags was decreased in the urine and all compartments of the bladder (Fig. 5F and G), while host innate defenses have been shown to be induced and engaged (23). The data reconfirmed that only 0.1 to 1% of invasive events lead to the formation of an IBC, perhaps as a result of TLR4-mediated bacterial expulsion (46). Furthermore, the wide range of unique tags present in the intracellular compartment at 6 hpi (Fig. 5G) corresponded with the natural variation in IBC number between mice, correlating with our earlier results (Fig. 2).

Between 6 and 24 hpi, the bacterial tags detected in the kidneys decreased (Fig. 5H). However, the tags detected in the bladder lumen and intracellular bladder fractions increased (Fig. 5F and G), suggesting that the overall bacterial diversity of the bladder was increasing due to shedding of bacteria carrying independent, unique tags from the kidney. In order to understand the overlap of bacteria in different niches, the identities of each tag were determined in each niche at each time point. We then determined on a per-mouse basis the fraction of unique and shared tags present within and between the following niches: urine, bladder lumen, bladder epithelium, and kidneys. For each time point, we determined the fraction and identity of each tagged strain present in each of the 15 possible overlapping and distinct niche combinations out of the total number of tags present within the urinary tract (Fig. 5I to M). At 6 hpi, the kidneys and urine contained 34% of bacterial

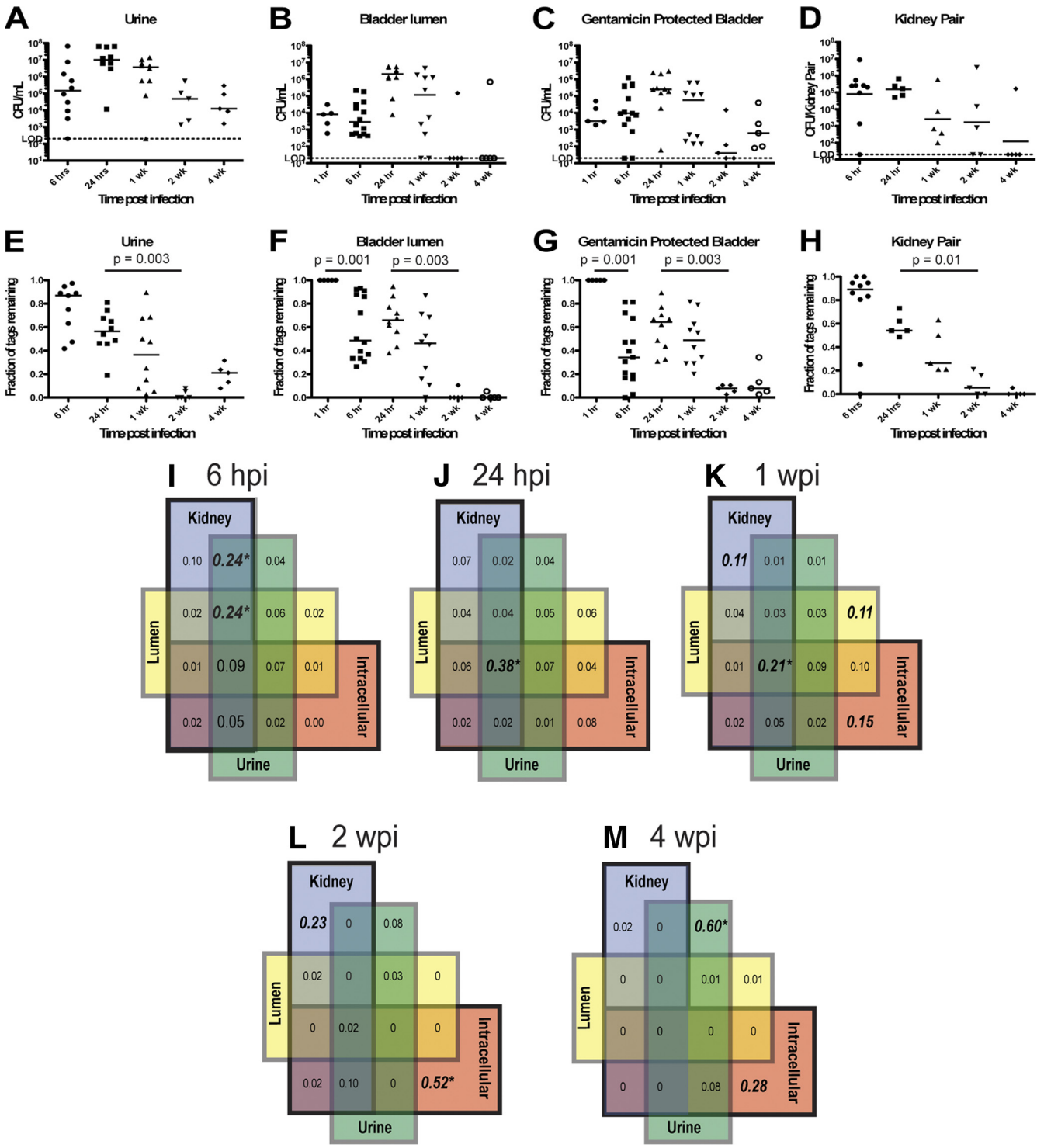

FIG. 5. Niche-specific diversity over time demonstrates population dynamics throughout UTI. At the indicated times postinfection, urine was obtained via gentle suprapubic pressure and plated to enumerate CFU (A) and the fraction of tags remaining (E). A gentamicin protection assay was performed to enumerate luminal CFU (B) and the fraction of tags remaining (F) and gentamicin-protected CFU (C) and tags remaining (G). Kidneys were also plated to enumerate CFU (D) and tags remaining (H). The niche occupation of specific tags was determined and is represented as the average fraction of tags present in distinct and overlapping niches (15 total permutations) and displayed as a 4-set Venn diagram at 6 hpi (I), 24 hpi (J), 1 wpi (K), 2 wpi (L), and 4 wpi (M). Each percentage listed displays the fraction of tags present in that unique or shared niche out of the total number of tags in each murine urinary tract. Data for panels A to H represent 1 to 3 experiments, with 5 mice per time point. Data for panels I to M represent experiments where kidney information was available: 2 experiments with 4 or 5 mice for panel I and 1 experiment with 5 mice each for panels J to M. *, the niche combination with the greatest unique diversity present. Bars are median values. *P* values were calculated using a two-tailed Mann-Whitney nonparametric comparison.

diversity not present in a bladder niche, likely reflecting the population that gained access to the kidney earlier in the infection as a result of VUR. At 24 hpi, 38% of the total tagged strains still present within the urinary tract were shared between all of the compartments (Fig. 5J). These data show that at 24 hpi, the majority of individual clones of bacteria are populating every niche within the urinary tract, likely as a result of emergence from IBCs earlier in infection and descent from the kidneys to seed other niches of the urinary tract.

By 48 hpi, the CFU in the bladder stratified into a bimodal distribution reflecting the development of persistent bacteriuria and bladder titers of $>10^4$ CFU or resolution of bacteriuria and establishment of QIRs with UPEC titers of $<10^4$ CFU (20, 40). The bimodal distribution was evident in the bladder lumen and gentamicin-protected fractions at 1 wpi (Fig. 5C). At 2 wpi in this experimental set, bacteria were no longer present in the lumen and urine in 4/5 of the mice and instead exclusively occupied gentamicin-protected reservoirs within the bladder epithelium or kidney (Fig. 5L). At 1 wpi, among the mice with high bladder bacterial counts indicative of chronic cystitis, 21% of the tags were shared in all niches. In contrast, 15% of the tags remaining in mice that resolved bacteriuria and formed QIRs were located exclusively in a gentamicin-protected niche, which increased to 28% of all urinary tract diversity by 4 wpi (Fig. 5K and M). The majority of tags at 4 wpi (60%) were present only in the urine without a bladder or kidney niche colonized, potentially suggesting that these bacteria colonized the ureter, urethra, or periurethral area, explaining why they were not found in another niche (Fig. 5M). The lumen in these mice was not colonized with bacteria, while the gentamicin-protected fraction had 10^3 CFU, suggesting that these mice were resolved with QIR formation. Thus, at different times during the infection, the urine fraction contains bacteria shed from the kidneys, planktonic bacteria from the bladder lumen, bacteria strongly adhered to or within exfoliated epithelial cells, or bacteria otherwise lost from bladder and kidney niches (Fig. 5I to M).

DISCUSSION

We created 40 isogenic uniquely tagged UPEC strains and assessed the presence of these bacteria in niches within the urinary tract over time with a multiplex PCR assay. This approach allowed us to provide an accurate accounting of the strains distributed throughout different compartments in the urinary tract over the course of UTI. By recovering bacteria from the samples on agar overnight to amplify even rare genetic tags, our approach resulted in a highly sensitive assay that provided a conservative estimate of the strains present in each compartment and their distributions throughout the urinary tract at the time of sampling. Using this molecular approach to better understand the obstacles in UPEC pathogenesis, we have revealed a series of population bottlenecks and interactions between distinct populations of the bladder and kidneys that impact the dynamics of the UPEC population during infection as a whole.

When C3H/HeN mice are inoculated with 10^7 CFU UTI89, 10^3 to 10^4 CFU invade the bladder epithelium at 1 hpi, and all of bacterial tags can be accounted for in the bladder intracellular population (Fig. 5G). Subsequently, 3 to 700 IBCs are formed per bladder by 6 hpi, and as demonstrated herein, each IBC is derived from a single bacterium that enters into the cytoplasm of a superficial facet cell (Fig. 1 and 2). Together, 0.1% of the inoculum invades the epithelium, and <2% of the invasive bacteria successfully form IBCs. The most stringent population bottleneck observed is between 1 and 24 hpi, corresponding to the time frame when a limited number of invasive bacteria have entered into the IBC cycle while innate immunity is engaged to clear luminal organisms. These dynamics produce a founder effect. The variance of the fraction of tags present within the bladder epithelium at 6 hpi and in the whole bladder at 24 hpi (Fig. 2, 3C, 5G) reflects the large bladder-to-bladder variance in IBC numbers and begins to reflect the bimodal distribution in infection outcome. The cause of the variance in IBC numbers is unknown but presumably reflects factors necessary to penetrate the various bottlenecks described here.

Our experimental data demonstrating the clonality of IBCs suggest that IBC formation with a concurrent reduction of the luminal UPEC population places a significant constraint on the number of organisms progressing through to later stages of infection. Indeed, modeling clonal IBC formation as the only pathway by which organisms can persist in the urinary tract fits the observed data very well and supports this hypothesis (see Fig. S1 in the supplemental material). Given that IBCs are clonal, a single IBC can contribute only to the detection of a single tag. So long as a tag is detected in our PCR assay, we cannot distinguish whether it was present in one or many IBCs. Therefore, assuming that tags are equivalent and detection by PCR is efficient, this is akin to an experiment where for every IBC, a die with 40 different numbers (each corresponding to a tag) is cast, and we count how many different numbers were thrown as a result of all casts of the die. With these assumptions, the probability distribution of the number of tags detected (different numbers of the die) given a number of IBCs formed (number of casts of the die) can be calculated exactly using a multinomial distribution (see Fig. S1 in the supplemental material). If there are other pathways to persistence that do not involve IBC formation (such as persistence exclusively in the lumen of the bladder), the number of tags detected can be modeled as additional throws of the die, 1 per each additional extracellular clone (see Fig. S1A in the supplemental material). Given the close fit between the multinomial expectation (based solely on IBC number) and the observed number of tags (Fig. 2), if there is another pathway to persistence, its contributions in terms of diversity are very small and effectively not measurable in our data. Small, exclusively luminal populations (not necessarily clonally derived from a single founder) could be predicted to drastically increase the expected fraction of tags persisting when low numbers of IBCs are present, though this is not experimentally observed (see Fig. S1A and Fig. S2 in the supplemental material). Although it is formally possible that clonal, extracellular populations contribute to bacterial diversity within the bladder at 6 hpi, the most likely interpretation of our data is that by 24 hpi, the extracellular population is largely a subset of bacteria arising from bacterial subpopulations that have emerged from other niches, with IBCs being a major source (Fig. 5I and J).

The outcomes of acute infection are (i) resolution of bacteriuria which can be accompanied by the formation of a QIR,

which can lead to recurrent infection, or (ii) chronic active cystitis marked by persistent bacteriuria for >7 months, which presumably reflects extracellular replication of bacteria (20, 40). Our data described above indicate that the strongest population bottlenecks exist within the first 24 hpi. Prior studies of UPEC mutants with defects in IBC development suggest that the first-generation IBCs are important for the establishment of acute cystitis (25, 48).

The studies presented herein have several key implications. First, in species such as humans, where isolated cystitis is common, the bottlenecks due to invasion and the IBC cycle may be even more stringent than observed in our studies in C3H/HeN mice, because there may be no mixing of bacteria being shed from the kidneys into the bladder. Inhibitors at the point of the major bottlenecks within the first 24 h of infection may significantly attenuate infection, both acute and chronic. For instance, inhibition of the IBC pathway, either by blocking IBC formation, development, or dispersal, may alter outcomes by reducing the number of QIRs and limiting chronic active cystitis. Combined with a FimH vaccine, invasion inhibitors may be particularly potent in preventing and treating UTI (19). A recent study showed that in a urological cohort of women, UPEC strains isolated from urine from 6/8 patients were not actively expressing type 1 pili (18). Our results (Fig. 5M) that 60% of strains detected were present only in the urine argue that these UPEC may indeed reflect strains lost from the bladder, as they were not detectable in any other urinary tract niche. Thus, although it is possible that these strains are not expressing type 1 pili as suggested by the results of Hagan et al. (18), their existence presumably depended on earlier colonization events involving type 1 pili and other virulence factors. Finally, the development and maintenance of genomic changes by UPEC during UTI may be contingent on the timing of acquisition of mutations, rearrangements, or deletions in the genome due to the bottleneck constraints present in the system. For instance, a mutant subpopulation obtaining antimicrobial resistance to trimethoprim through a mutation in dihydrofolate reductase (DHFR) may be extinguished by a stringent stochastic bottleneck even under circumstances when the antibiotic is being administered and an antibiotic resistance mutation provides a selective advantage. This would be expected to occur if the proportion of the population with that advantage is sufficiently too small to overcome the inherent stochastic barriers that eliminate the vast majority of the population and produce a founder effect, likely in this case to arise from majority members that do not have the advantageous mutation. Alternatively, hosts in which bacteria more effectively penetrate the early bottlenecks, such as those developing chronic cystitis where diversity is maintained, may provide productive environments for the selection and perpetuation of adaptive mutations. Thus, diversity and selective evolution may be constrained by these stochastic mechanisms during cystitis and/or dramatically favor mutations that facilitate invasion and IBC formation. Indeed, several genes important for invasion, IBC formation, and living within host cells were shown to be under positive selection in UPEC (5, 6).

The findings herein present the hypothesis that an increased number of IBCs activates a host immune response that predisposes to persistent bacteriuria and chronic cystitis. In C3H/HeN mice, increasing the inoculum to 10^8 CFU/ml increases the average number of IBCs formed and increases the percentage of mice experiencing persistent bacteriuria (20). Currently, it is not possible to evaluate these metrics of infection within the same mouse. Longitudinal monitoring of bacterial populations *in vivo* using techniques in development, such as intravital multiphoton microscopy to enumerate acute IBC formation at 6 hpi and determine bacteriuria and tissue titers at 2 wpi, will provide further resolution to the consequences of early infection events on subacute and chronic outcomes. Our findings are especially relevant for mucosal pathogens that have to transit through potential population bottlenecks similar to those described in this work (9, 27, 28). Finally, the methodology described herein could be ideal to analyze population bottlenecks, niche occupation, and clonality by other bacterial pathogens of mucosal sites.

ACKNOWLEDGMENTS

We thank Karen Dodson for critical review of the manuscript.

This work was supported fully or in part by the National Institutes of Health R01 DK51406 (S.J.H.), P50 DK64540 (S.J.H. and P.C.S.), and DK07444301 (P.C.S.).

REFERENCES

1. **Ali, A., et al.** 2006. Analysis of genetic bottlenecks during horizontal transmission of *Cucumber mosaic virus*. J. Virol. **80:**8345–8350.
2. **Anderson, G. G., et al.** 2003. Intracellular bacterial biofilm-like pods in urinary tract infections. Science **301:**105–107.
3. **Bergstrom, C. T., P. McElhany, and L. A. Real.** 1999. Transmission bottlenecks as determinants of virulence in rapidly evolving pathogens. Proc. Natl. Acad. Sci. U. S. A. **96:**5095–5100.
4. **Blango, M. G., and M. A. Mulvey.** 2010. Persistence of uropathogenic *Escherichia coli* in the face of multiple antibiotics. Antimicrob. Agents Chemother. **54:**1855–1863.
5. **Chen, S. L., et al.** 2009. Positive selection identifies an in vivo role for FimH during urinary tract infection in addition to mannose binding. Proc. Natl. Acad. Sci. U. S. A. **106:**22439–22444.
6. **Chen, S. L., et al.** 2006. Identification of genes subject to positive selection in uropathogenic strains of *Escherichia coli*: a comparative genomics approach. Proc. Natl. Acad. Sci. U. S. A. **103:**5977–5982.
7. **Chiang, S. L., and J. J. Mekalanos.** 1998. Use of signature-tagged transposon mutagenesis to identify *Vibrio cholerae* genes critical for colonization. Mol. Microbiol. **27:**797–805.
8. **Cusumano, C. K., C. S. Hung, S. L. Chen, and S. J. Hultgren.** 2010. Virulence plasmid harbored by uropathogenic *Escherichia coli* functions in acute stages of pathogenesis. Infect. Immun. **78:**1457–1467.
9. **Darwin, A. J., and V. L. Miller.** 1999. Identification of *Yersinia enterocolitica* genes affecting survival in an animal host using signature-tagged transposon mutagenesis. Mol. Microbiol. **32:**51–62.
10. **Datsenko, K. A., and B. L. Wanner.** 2000. One-step inactivation of chromosomal genes in *Escherichia coli* K-12 using PCR products. Proc. Natl. Acad. Sci. U. S. A. **97:**6640–6645.
11. **Ferry, S., S. Holm, H. Stenlund, R. Lundholm, and T. Monsen.** 2004. The natural course of uncomplicated lower urinary tract infection in women illustrated by a randomized placebo controlled study. Scand. J. Infect. Dis. **36:**296–301.
12. **Foxman, B.** 2002. Epidemiology of urinary tract infections: incidence, morbidity, and economic costs. Am. J. Med. **113**(Suppl. 1A)**:**5S–13S.
13. **Foxman, B.** 2010. The epidemiology of urinary tract infection. Nat. Rev. Urol. **7:**653–660.
14. **Garofalo, C. K., et al.** 2007. *Escherichia coli* from urine of female patients with urinary tract infections is competent for intracellular bacterial community formation. Infect. Immun. **75:**52–60.
15. **Gupta, K., T. M. Hooton, and W. E. Stamm.** 2001. Increasing antimicrobial resistance and the management of uncomplicated community-acquired urinary tract infections. Ann. Intern. Med. **135:**41–50.
16. **Gupta, K., T. M. Hooton, and W. E. Stamm.** 2005. Isolation of fluoroquinolone-resistant rectal *Escherichia coli* after treatment of acute uncomplicated cystitis. J. Antimicrob. Chemother. **56:**243–246.
17. **Gupta, K., D. F. Sahm, D. Mayfield, and W. E. Stamm.** 2001. Antimicrobial resistance among uropathogens that cause community-acquired urinary tract infections in women: a nationwide analysis. Clin. Infect. Dis. **33:**89–94.
18. **Hagan, E. C., A. L. Lloyd, D. A. Rasko, G. J. Faerber, and H. L. Mobley.** 2010. *Escherichia coli* global gene expression in urine from women with urinary tract infection. PLoS Pathog. **6:**e1001187.

19. **Han, Z., et al.** 2010. Structure-based drug design and optimization of mannoside bacterial FimH antagonists. J. Med. Chem. **53:**4779–4792.
20. **Hannan, T. J., I. U. Mysorekar, C. S. Hung, M. L. Isaacson-Schmid, and S. J. Hultgren.** 2010. Early severe inflammatory responses to uropathogenic *E. coli* predispose to chronic and recurrent urinary tract infection. PLoS Pathog. **6:**e1001042.
21. **Haraoka, M., et al.** 1999. Neutrophil recruitment and resistance to urinary tract infection. J. Infect. Dis. **180:**1220–1229.
22. **Hung, C. S., K. W. Dodson, and S. J. Hultgren.** 2009. A murine model of urinary tract infection. Nat. Protoc. **4:**1230–1243.
23. **Ingersoll, M. A., K. A. Kline, H. V. Nielsen, and S. J. Hultgren.** 2008. G-CSF induction early in uropathogenic *Escherichia coli* infection of the urinary tract modulates host immunity. Cell. Microbiol. **10:**2568–2578.
24. **Justice, S. S., et al.** 2004. Differentiation and developmental pathways of uropathogenic *Escherichia coli* in urinary tract pathogenesis. Proc. Natl. Acad. Sci. U. S. A. **101:**1333–1338.
25. **Justice, S. S., D. A. Hunstad, P. C. Seed, and S. J. Hultgren.** 2006. Filamentation by *Escherichia coli* subverts innate defenses during urinary tract infection. Proc. Natl. Acad. Sci. U. S. A. **103:**19884–19889.
26. **Ko, Y. C., et al.** 1993. Elevated interleukin-8 levels in the urine of patients with urinary tract infections. Infect. Immun. **61:**1307–1314.
27. **Kuss, S. K., C. A. Etheredge, and J. K. Pfeiffer.** 2008. Multiple host barriers restrict poliovirus trafficking in mice. PLoS Pathog. **4:**e1000082.
28. **Lancaster, K. Z., and J. K. Pfeiffer.** 2010. Limited trafficking of a neurotropic virus through inefficient retrograde axonal transport and the type I interferon response. PLoS Pathog. **6:**e1000791.
29. **Langermann, S., et al.** 1997. Prevention of mucosal *Escherichia coli* infection by FimH-adhesin-based systemic vaccination. Science **276:**607–611.
30. **Lehoux, D. E., and R. C. Levesque.** 2002. PCR screening in signature-tagged mutagenesis of essential genes. Methods Mol. Biol. **192:**225–234.
31. **Lehoux, D. E., F. Sanschagrin, and R. C. Levesque.** 1999. Defined oligonucleotide tag pools and PCR screening in signature-tagged mutagenesis of essential genes from bacteria. Biotechniques **26:**473–480.
32. **Lim, R.** 2009. Vesicoureteral reflux and urinary tract infection: evolving practices and current controversies in pediatric imaging. AJR Am. J. Roentgenol. **192:**1197–1208.
33. **Mabeck, C. E.** 1972. Treatment of uncomplicated urinary tract infection in non-pregnant women. Postgrad. Med. J. **48:**69–75.
34. **Martinez, J. J., M. A. Mulvey, J. D. Schilling, J. S. Pinkner, and S. J. Hultgren.** 2000. Type 1 pilus-mediated bacterial invasion of bladder epithelial cells. EMBO J. **19:**2803–2812.
35. **Masharsky, A. E., et al.** 2010. A substantial transmission bottleneck among newly and recently HIV-1-infected injection drug users in St. Petersburg, Russia. J. Infect. Dis. **201:**1697–1702.
36. **Mecsas, J.** 2002. Use of signature-tagged mutagenesis in pathogenesis studies. Curr. Opin. Microbiol. **5:**33–37.
37. **Mecsas, J., I. Bilis, and S. Falkow.** 2001. Identification of attenuated *Yersinia pseudotuberculosis* strains and characterization of an orogastric infection in BALB/c mice on day 5 postinfection by signature-tagged mutagenesis. Infect. Immun. **69:**2779–2787.
38. **Mulvey, M. A., et al.** 1998. Induction and evasion of host defenses by type 1-piliated uropathogenic *Escherichia coli*. Science **282:**1494–1497.
39. **Mulvey, M. A., J. D. Schilling, and S. J. Hultgren.** 2001. Establishment of a persistent *Escherichia coli* reservoir during the acute phase of a bladder infection. Infect. Immun. **69:**4572–4579.
40. **Mysorekar, I. U., and S. J. Hultgren.** 2006. Mechanisms of uropathogenic *Escherichia coli* persistence and eradication from the urinary tract. Proc. Natl. Acad. Sci. U. S. A. **103:**14170–14175.
41. **Oberle, M., O. Balmer, R. Brun, and I. Roditi.** Bottlenecks and the maintenance of minor genotypes during the life cycle of *Trypanosoma brucei*. PLoS Pathog. **6:**e1001023.
42. **Rosen, D. A., T. M. Hooton, W. E. Stamm, P. A. Humphrey, and S. J. Hultgren.** 2007. Detection of intracellular bacterial communities in human urinary tract infection. PLoS Med. **4:**e329.
43. **Rosen, D. A., C. S. Hung, K. A. Kline, and S. J. Hultgren.** 2008. Streptozocin-induced diabetic mouse model of urinary tract infection. Infect. Immun. **76:**4290–4298.
44. **Rosen, D. A., et al.** 2008. Utilization of an intracellular bacterial community pathway in *Klebsiella pneumoniae* urinary tract infection and the effects of FimK on type 1 pilus expression. Infect. Immun. **76:**3337–3345.
45. **Russo, T. A., A. Stapleton, S. Wenderoth, T. M. Hooton, and W. E. Stamm.** 1995. Chromosomal restriction fragment length polymorphism analysis of *Escherichia coli* strains causing recurrent urinary tract infections in young women. J. Infect. Dis. **172:**440–445.
46. **Song, J., et al.** 2009. TLR4-mediated expulsion of bacteria from infected bladder epithelial cells. Proc. Natl. Acad. Sci. U. S. A. **106:**14966–14971.
47. **Svanborg Eden, C., D. Briles, L. Hagberg, J. McGhee, and S. Michalec.** 1985. Genetic factors in host resistance to urinary tract infection. Infection **13**(Suppl. 2)**:**S171–S176.
48. **Wright, K. J., P. C. Seed, and S. J. Hultgren.** 2007. Development of intracellular bacterial communities of uropathogenic *Escherichia coli* depends on type 1 pili. Cell. Microbiol. **9:**2230–2241.
49. **Wright, K. J., P. C. Seed, and S. J. Hultgren.** 2005. Uropathogenic *Escherichia coli* flagella aid in efficient urinary tract colonization. Infect. Immun. **73:**7657–7668.

Editor: S. M. Payne